

---

1 **High secondary formation of nitrogen-containing organics (NOCs) and its**  
2 **possible link to oxidized organics and ammonium**

3 Guohua Zhang<sup>1</sup>, Xiufeng Lian<sup>1,2</sup>, Yuzhen Fu<sup>1,2</sup>, Qin hao Lin<sup>1</sup>, Lei Li<sup>3</sup>, Wei Song<sup>1</sup>, Zhanyong  
4 Wang<sup>4</sup>, Mingjin Tang<sup>1</sup>, Duohong Chen<sup>5</sup>, Xinhui Bi<sup>1,\*</sup>, Xinming Wang<sup>1</sup>, Guoying Sheng<sup>1</sup>

5

6 <sup>1</sup> State Key Laboratory of Organic Geochemistry and Guangdong Key Laboratory of  
7 Environmental Resources Utilization and Protection, Guangzhou Institute of Geochemistry,  
8 Chinese Academy of Sciences, Guangzhou 510640, PR China

9 <sup>2</sup> University of Chinese Academy of Sciences, Beijing 100039, PR China

10 <sup>3</sup> Institute of Mass Spectrometer and Atmospheric Environment, Jinan University, Guangzhou  
11 510632, PR China

12 <sup>4</sup> School of Intelligent Systems Engineering, Sun Yat-sen University, Shenzhen 518107, PR  
13 China

14 <sup>5</sup> State Environmental Protection Key Laboratory of Regional Air Quality Monitoring,  
15 Guangdong Environmental Monitoring Center, Guangzhou 510308, PR China

16

17 Correspondence to: Xinhui Bi (bixh@gig.ac.cn)

18

---

19 **Highlights**

- 20 ● Nitrogen-containing organics (NOCs) were highly internally mixed with photochemically  
21 produced secondary oxidized organics
- 22 ● NOCs could be well predicted by the variations of these oxidized organics and ammonium
- 23 ● Higher relative humidity and NO<sub>x</sub> may facilitate the conversion of these oxidized organics  
24 to NOCs

---

25        **Abstract**

26        Nitrogen-containing organic compounds (NOCs) substantially contribute to light  
27        absorbing organic aerosols, although the atmospheric processes responsible for the secondary  
28        formation of these compounds are poorly understood. In this study, seasonal atmospheric  
29        processing of NOCs were investigated by single particle mass spectrometry in urban  
30        Guangzhou from 2013-2014. The relative abundance of NOCs is found to be strongly enhanced  
31        when internal mixed with the photochemically produced secondary oxidized organics (i.e.,  
32        formate, acetate, pyruvate, methylglyoxal, glyoxylate, oxalate, malonate and succinate) and  
33        ammonium. In addition, both the hourly detected particle number and relative abundance of  
34        NOCs are highly correlated with those of secondary oxidized organics and ammonium. It is  
35        therefore hypothesized that secondary formation of NOCs most likely links to the oxidized  
36        organics and ammonium. Results from both multiple linear regression analysis and positive  
37        matrix factorization analysis further show that the relative abundance of NOCs could be well  
38        predicted ( $R^2 > 0.7$ ,  $p < 0.01$ ) by the oxidized organics and ammonium. Interestingly, the  
39        relative abundance of NOCs is inversely correlated with ammonium, whereas their number  
40        fractions are positively correlated. This result suggests that although the formation of NOCs  
41        does require the involvement of  $\text{NH}_3/\text{NH}_4^+$ , the relative amount of ammonium may have a  
42        negative effect. The conversion of oxidized organics to NOCs is likely facilitated by higher  
43        humidity and  $\text{NO}_x$ . Due to the relatively high oxidized organics and  $\text{NH}_3/\text{NH}_4^+$ , the relative  
44        contributions of NOCs in summer and autumn were higher than those in spring and winter. To  
45        the best of our knowledge, this is the first direct field observation study reporting a close

---

46 association between NOCs and both oxidized organics and ammonium. These findings have  
47 substantial implications for the role of ammonium in the atmosphere, particularly in models  
48 that predict the evolution and deposition of NOCs.

49

50 **Keywords:** nitrogen-containing organic compounds, individual particles, oxidized organics,  
51 ammonium, mixing state, single particle mass spectrometry

---

## 53 **1 Introduction**

54       Organic aerosols that strongly absorb solar radiation are referred to as brown carbon  
55 (BrC), capable of a comparable level of light absorption in the spectral range of near-  
56 ultraviolet (UV) light as black carbon (Andreae and Gelencser, 2006; Feng et al., 2013; Yan  
57 et al., 2018). Nitrogen-containing organic compounds (NOCs) substantially contribute to the  
58 pool of BrC (Feng et al., 2013; Mohr et al., 2013; Li et al., 2019), and have a major effect  
59 on atmospheric chemistry, human health and climate forcing (Noziere et al., 2015;  
60 Kanakidou et al., 2005; Shrivastava et al., 2017; De Gouw and Jimenez, 2009). The  
61 particulate organic nitrogen accounts for a large fraction of total airborne nitrogen (~30%),  
62 although the proportion exhibits a high variability temporally and spatially, and therefore  
63 has an influence on both regional and global N deposition (Neff et al., 2002; Shi et al., 2010;  
64 Cape et al., 2011). However, the sources, evolution and optical properties of NOCs remain  
65 unclear and contribute significantly to uncertainties in the estimation of their impacts on the  
66 environment and climate (Laskin et al., 2015; Feng et al., 2013).

67       NOCs are ubiquitous components of atmospheric aerosols, cloud water and rainwater  
68 (Altieri et al., 2009; Desyaterik et al., 2013; Laskin et al., 2015), spanning a wide range of  
69 molecular weights, structures and light absorption properties (Lin et al., 2016). Emissions of  
70 primary NOCs have been attributed to biomass burning, coal combustion, vehicle emissions,  
71 biogenic production and soil dust (Laskin et al., 2009; Desyaterik et al., 2013; Sun et al.,  
72 2017; Mace et al., 2003; Rastogi et al., 2011; Wang et al., 2017). A growing body of evidence

---

73 from laboratory studies suggests that secondary NOCs may be produced in gas phase,  
74 aerosol, and clouds. Maillard reactions involving mixtures of atmospheric aldehydes (e.g.,  
75 methylglyoxal/glyoxal) and ammonium/amines are of particular interests (e.g., Hawkins et  
76 al., 2016; De Haan et al., 2017; De Haan et al., 2011). A significant portion of NOCs may  
77 also be derived from the heterogeneous ageing of secondary organic aerosol (SOA) with  
78  $\text{NH}_3 / \text{NH}_4^+$  (Liu et al., 2015; Laskin et al., 2015). Mang et al. (2008) proposed that even  
79 trace levels of ammonia may be sufficient to form NOCs via this pathway. In addition, gas  
80 phase formation of NOCs through interaction between volatile organic hydrocarbons and  
81  $\text{NO}_x$  and other oxidations, followed by condensation may have potential contribution (Fry  
82 et al., 2014; Stefenelli et al., 2019; Lehtipalo et al., 2018).

83       The secondary formation of NOCs is especially prevalent in environments experiencing  
84 high anthropogenic emissions (Yu et al., 2017; Ho et al., 2015), although further studies are  
85 required to comprehensively establish the formation mechanisms. A major obstacle is that  
86 organic and inorganic matrix effects have a profound impact on the chemistry of organic  
87 compounds in bulk aqueous particles and particles undergoing drying (El-Sayed et al., 2015;  
88 Lee et al., 2013). While real-time characterization studies remain a challenge due to the  
89 extremely complex chemical nature of NOCs, establishing this data along with the co-  
90 variation of NOCs with other chemical components would help to identify the sources and  
91 evolution of NOCs. Using single-particle aerosol time-of-flight mass spectrometry, Wang et  
92 al. (2010) observed that the widespread occurrence of NOCs was closely correlated with  
93 particle acidity in the atmosphere of Shanghai (China). In addition, real-time measurements

---

94 of the atmosphere in New York (US) by aerosol mass spectrometry indicated a positive link  
95 between the age of organic species and the N/C ratio (Sun et al., 2011). Further in-depth  
96 studies are required to identify the role of formation conditions (e.g., relative humidity (RH)  
97 and pH) for secondary NOCs (Aiona et al., 2017; Nguyen et al., 2012). In present study, the  
98 mixing state of individual particles were investigated, involving NOCs, oxidized organics  
99 and ammonium, based on on-line seasonal observations using a single particle aerosol mass  
100 spectrometry (SPAMS). Our findings show that the formation of NOCs is significantly  
101 linked to oxidized organics and  $\text{NH}_4^+$ , which has important environmental implications for  
102 assessing the impact and fate of these compounds.

103

## 104 **2 Methods**

### 105 **2.1 Field measurements**

106 Sampling was performed at the Guangzhou Institute of Geochemistry, a representative  
107 urban site in Guangzhou (China), a megacity in the Pearl River Delta (PRD) region. SPAMS  
108 analysis was performed (Hexin Analytical Instrument Co., Ltd., China) to establish the size  
109 and chemical composition of individual particles in real-time (Li et al., 2011). The sampling  
110 inlet for aerosol characterization was situated 40 meters above the ground level. A brief  
111 description of the performance of SPAMS and other instruments can be found in the  
112 Supporting Information. The sampling periods covered four seasons including spring (21/02  
113 to 11/04 2014), summer (13/06 to 16/07 2013), autumn (26/09 to 19/10 2013) and winter  
114 (15/12 to 25/12 2013). The total measured particle numbers and mean values for

---

115 meteorological data and gaseous pollutants, are outlined for each season in Table S1 and  
116 were described in a previous publication (Zhang et al., 2019).

117

## 118 **2.2 SPAMS data analysis**

119 Fragments of NOCs were identified according to detection of ion peaks at  $m/z$  -26  $[\text{CN}]^-$   
120 or -42  $[\text{CNO}]^-$ , generally due to the presence of C-N bonds (Silva and Prather, 2000;  
121 Zawadowicz et al., 2017; Pagels et al., 2013). Laboratory produced C-N bonds compounds  
122 from bulk solution-phase reactions between the representative oxidized organics (i.e.,  
123 methylglyoxal) and ammonium sulfate was used to confirm the generation of ion peaks at  
124  $m/z$  -26  $[\text{CN}]^-$  and/or -42  $[\text{CNO}]^-$  using SPAMS (Fig. S1). Thus, the NOCs herein may refer  
125 to complex nitrated organics such as organic nitrates, nitro-aromatics, nitrogen heterocycles  
126 and polyphenols. Unfortunately, how well  $[\text{CN}]^- / [\text{CNO}]^-$  ions could represent NOCs cannot  
127 be quantified, although they were the most commonly reported NOCs peaks by single  
128 particle mass spectrometry (Silva and Prather, 2000; Zawadowicz et al., 2017; Pagels et al.,  
129 2013). In the present study,  $[\text{CN}]^- / [\text{CNO}]^-$  ions are among the major peaks detected by the  
130 SPAMS (Fig. 1). A rough estimate from the peak area ratio of  $[\text{CN}]^- / [\text{CNO}]^-$  ions and the  
131 most likely NOCs fragments (i.e., various amines, and an entire series of nitrogen-containing  
132 cluster ions  $\text{C}_n\text{N}^-$ ,  $n = 1, 2, 3, \dots$ ) (Silva and Prather, 2000) shows that  $[\text{CN}]^- / [\text{CNO}]^-$  ions  
133 may represent more than 90% of these NOCs peaks. The number fractions (Nfs) of particles  
134 that contained NOCs ranged from 56-59% across all four seasons (Table S1). The number  
135 of detected NOCs-containing particles distributing along their vacuum aerodynamic



---

136 diameter ( $d_{va}$ ) is shown in Fig. S2. Most of the detected NOC-containing particles had a  $d_{va}$   
137 in a range of 300-1200 nm.

138 A representative mass spectrum for NOCs-containing particles is shown in Fig. 1.  
139 Dominant peaks in the mass spectrum were 39 [K]<sup>+</sup>, 23 [Na]<sup>+</sup>, nitrate (-62 [NO<sub>3</sub>]<sup>-</sup> or -46  
140 [NO<sub>2</sub>]<sup>-</sup>), sulfate (-97 [HSO<sub>4</sub>]<sup>-</sup>), organics (27 [C<sub>2</sub>H<sub>3</sub>]<sup>+</sup>, 63 [C<sub>5</sub>H<sub>3</sub>]<sup>+</sup>, -42 [CNO]<sup>-</sup>, -26 [CN]<sup>-</sup>),  
141 ammonium (18 [NH<sub>4</sub>]<sup>+</sup>) and carbon ion clusters (C<sub>n</sub><sup>+/-</sup>, n = 1, 2, 3,...). NOCs-containing  
142 particles were internally mixed with various oxidized organics, represented as formate at m/z  
143 -45 [HCO<sub>2</sub>]<sup>-</sup>, acetate at m/z -59 [CH<sub>3</sub>CO<sub>2</sub>]<sup>-</sup>, methylglyoxal at m/z -71 [C<sub>3</sub>H<sub>3</sub>O<sub>2</sub>]<sup>-</sup>, glyoxylate  
144 at m/z -73 [C<sub>2</sub>HO<sub>3</sub>]<sup>-</sup>, pyruvate at m/z -87 [C<sub>3</sub>H<sub>3</sub>O<sub>3</sub>]<sup>-</sup>, malonate at m/z -103 [C<sub>3</sub>H<sub>3</sub>O<sub>4</sub>]<sup>-</sup> and  
145 succinate at m/z -117 [C<sub>4</sub>H<sub>5</sub>O<sub>4</sub>]<sup>-</sup> (Zhang et al., 2017; Zauscher et al., 2013; Lee et al., 2003).  
146 These oxidized organics showed their pronounced diurnal trends with afternoon maximum,  
147 and were highly correlated ( $r = 0.72 - 0.94$ ,  $p < 0.01$ ) with each other. Therefore, they were  
148 primarily attributed to secondary oxidized organics from photochemical oxidation products  
149 of various volatile organic compounds (VOCs) (Paulot et al., 2011; Zhao et al., 2012; Ho et  
150 al., 2011), and the details can be found in our previous publication (Zhang et al., 2019). More  
151 information on the seasonal variation range of the Nfs of oxidized organics, ammonium and  
152 NOCs is presented in Fig. S3.

153 Hourly mean Nfs and relative peak areas were applied herein to indicate the variations  
154 of aerosol compositions in individual particles. Even though advances have been made in  
155 the quantification of specific chemical species for individual particles based on their  
156 respective peak area information, it is still quite a challenge for SPAMS to provide

---

157 quantitative information on aerosol components mainly due to matrix effects, incomplete  
158 ionization and so forth (Qin et al., 2006; Jeong et al., 2011; Healy et al., 2013; Zhou et al.,  
159 2016). Despite of this, the variation of relative peak area should be a good indicator for the  
160 investigation of atmospheric processing of various species in individual particles (Wang et  
161 al., 2010; Zauscher et al., 2013; Sullivan and Prather, 2007; Zhang et al., 2014).

162

### 163 **3 Results and Discussion**

#### 164 **3.1 Evidence for the formation of NOCs from oxidized organics and ammonium**

165 Figure 2 shows the seasonal variations in Nfs of the oxidized organics and ammonium,  
166 which were internally mixed with NOCs. On average, more than 90% of the oxidized  
167 organics and 65% of ammonium (except spring) were found to be internally mixed with  
168 NOCs (Fig. S4). Regarding that the Nfs of NOCs relative to all the measured particles was  
169 ~60%, it could be concluded that NOCs were enhanced with the presence of oxidized  
170 organics and ammonium, with the enhancement associated with oxidized organics being the  
171 most pronounced.

172 A strong correlation between both the Nfs and relative peak areas (RPAs) of NOCs and  
173 oxidized organics further demonstrates their close associations, as shown in Fig. 3.  
174 Compared with the oxidized organics, the Nfs of ammonium-containing particles internally  
175 mixed with NOCs varied within a wider range (~40-90%). However, there is still an  
176 enhancement mixing of NOCs with ammonium. A positive correlation ( $R^2 = 0.50$ ,  $p < 0.01$ )  
177 is observed between the hourly detected number of NOCs and ammonium. It is worth noting

---

178 that a negative correlation ( $R^2 = 0.55, p < 0.01$ ) is obtained between the hourly average RPAs  
179 of NOCs and ammonium (Fig. 3).

180 Based on both the enhancement of NOCs and the high correlations with oxidized  
181 organics and ammonium, it is hypothesized that interactions between oxidized organics and  
182 ammonium contributed to the observed NOCs. Actually, formation of NOCs from  
183 ammonium and carbonyls has been confirmed in several laboratory studies (Sareen et al.,  
184 2010; Shapiro et al., 2009; Noziere et al., 2009; Kampf et al., 2016; Galloway et al., 2009).  
185 Secondary organic aerosols (SOA) produced from a large group of biogenic and  
186 anthropogenic VOCs can be further aged by  $\text{NH}_3/\text{NH}_4^+$  to generate NOCs (Nguyen et al.,  
187 2012; Bones et al., 2010; Updyke et al., 2012; Liu et al., 2015; Huang et al., 2017). In a  
188 chamber study, the formation of NOCs is enhanced in a  $\text{NH}_3$ -rich environment (Chu et al.,  
189 2016). While such chemical mechanisms might be complex, the initial steps generally  
190 involve reactions forming imines and amines, which can further react with carbonyl SOA  
191 compounds to form more complex products (e.g., oligomers/BrC) (Laskin et al., 2015).

192 To verify this hypothesis, multiple linear regression analysis is performed to test how  
193 well the RPAs of NOCs could be predicted by the oxidized organics and ammonium. As  
194 expected, there is a close association ( $R^2 = 0.71, p < 0.01$ ) between the predicted RPAs and  
195 the observed values of NOCs (Fig. 4), which supports this hypothesis. An obvious  
196 improvement in  $R^2$  implies that a model that uses both oxidized organics and ammonium to  
197 predict RPAs of NOCs is substantially better than one that uses only one predictor (either  
198 oxidized organics or ammonium in Fig. 3). The result indicates that interactions involving

---

199 oxidized organics and ammonium could explain over half of the observed variations in  
200 NOCs in the atmosphere of Guangzhou. A fraction of the unaccounted NOCs could be due  
201 to primary emissions and other formation pathways. This hypothesis could also be supported  
202 by the similar pattern of diurnal variation observed for NOCs and oxidized organics (Fig.  
203 S5), although there is a slight lag for the NOCs. Such diurnal pattern is similar to those  
204 observed in Beijing and Uintah (Yuan et al., 2016; Zhang et al., 2015). Notably, such diurnal  
205 pattern of secondary NOCs is effectively modelled when the production of NOCs via  
206 carbonyls and ammonium is included (Woo et al., 2013). In addition to possible photo-  
207 bleaching (Zhao et al., 2015), the lower contribution of NOCs during daytime may be partly  
208 explained by the lower RH, as discussed in section 3.2.

209 Interestingly, the relationship between NOCs and ammonium is distinctly different from  
210 the relationship between NOCs and oxidized organics (Fig. 3). This implies that the  
211 controlling factors on the formation of NOCs from ammonium are different from oxidized  
212 organics. On one hand, the positive correlation between the detected numbers reflects that  
213 the formation of NOCs does require the participant of  $\text{NH}_3/\text{NH}_4^+$ , consistent with the  
214 enhancement of NOCs in ammonium-containing particles discussed above. On the other  
215 hand, the negative correlation between the RPAs signifies that particles with higher relative  
216 ammonium content may inhibit the formation of NOCs. Consistently, there is a negative  
217 correlation between concentrations of WSON and  $\text{NH}_4^+$  in filter samples (Fig. S6). This is  
218 supported by the inverse correlation between that Nfs of ammonium that internally mixed  
219 with NOCs and the RPAs of ammonium (Fig. S7). This is also theoretically possible since

---

220 the formation of NOCs may be influenced by particle acidity (Miyazaki et al., 2014; Aiona  
221 et al., 2017; Nguyen et al., 2012), which is substantially affected by the abundance of  
222 ammonium. Particle acidity could also play a significant role in the gas-to-particle  
223 partitioning of aldehydes (Herrmann et al., 2015; Liggio et al., 2005; Gen et al., 2018; De  
224 Haan et al., 2018; Kroll et al., 2005), precursors for the formation of oxidized organics.  
225 Consistently, higher relative acidity was observed for the internally mixed ammonium and  
226 NOCs particles, compared to ammonium-containing particles without NOCs (Fig. S6), and  
227 thus may influence the formation of NOCs (Fig. S7). However, the higher relative acidity  
228 might also be a result of NOCs formation. A model simulation shows that after including the  
229 chemistry of SOA ageing with NH<sub>3</sub>, an increase in aerosol acidity would be expected due to  
230 the reduction in ammonium (Zhu et al., 2018). It is also noted that the particle acidity is  
231 roughly estimated by the relative abundance of ammonium, nitrate, and sulfate in individual  
232 particles (Denkenberger et al., 2007), and thus may not be representative of actual aerosol  
233 acidity or pH (Guo et al., 2015; Hennigan et al., 2015; Murphy et al., 2017). In addition,  
234 ammonia in gas phase is also efficient at producing NOCs (Nguyen et al., 2012), which may  
235 play a complex role in the distribution of ammonium and NOCs in particulate phase. The  
236 formation of ammonium and NOCs would compete for ammonia, which may also potentially  
237 result in the negative correlation between the RPAs of NOCs and ammonium. Unfortunately,  
238 such a role remains unclear since the variations of ammonia were not available in the present  
239 study.

240

---

### 241 3.2 Factors contributing to the NOCs resolved by positive matrix factorization (PMF)

#### 242 analysis

243 Figure 5 presents the PMF factor profiles obtained from the PMF model analysis  
244 (detailed information is provided in the SI) (Norris et al., 2009) and their diurnal variations.  
245 Around 75% of NOCs could be well explained by two factors, with 33% of the PMF resolved  
246 NOCs mainly associated with ammonium and carbonaceous ion peaks (ammonium factor),  
247 while 59% were mainly associated with oxidized organics (oxidized organics factor). The  
248 explained fraction of NOCs by the ammonium and oxidized organic factors is consistent  
249 with the linear regression analysis. In addition, PMF analysis provided information on the  
250 factor contribution and diurnal variations, which may help explain the seasonal variations  
251 and processes of NOCs. The ammonium factor showed a diurnal variation pattern peaking  
252 during early morning, which is consistent with the diurnal variation in RH (Zhang et al.,  
253 2019). This factor contributed to ~80% (Fig. S8) of the PMF resolved NOCs during spring  
254 with the highest RH (Table S1), whereas the oxidized organics factor dominated (> 80%) in  
255 summer and fall. In winter, these two factors similarly contributed (~40%). This may  
256 indicate a potential role of aqueous pathways in the formation of NOCs, particularly during  
257 spring. Differently, the oxidized organics factor showed a pattern of diurnal variation,  
258 increasing from morning hours and peaking overnight, which may correspond to the  
259 photochemical production of oxidized organics and followed interactions with condensed  
260 ammonium. This pathway may explain the slightly late peaking of NOCs compared to  
261 oxidized organics, as ammonium condensation is favorable overnight (Hu et al., 2008).

---

262 While there were similarities in the fractions of oxidized organics in the oxalate factor and  
263 the oxidized organics factor, they only contributed to 8% of the PMF resolved NOCs in the  
264 oxalate factor, which contained ~80% of the PMF resolved oxalate. As previously discussed,  
265 these oxidized organics are also precursors for the formation of oxalate (Zhang et al., 2019).  
266 Therefore, the PMF results suggest that there are two competitive pathways for the evolution  
267 of these oxidized organics. Some oxidized organics formed from photochemical activities  
268 were further oxidized to oxalate, resulting in a diurnal pattern of variation with concentration  
269 peaks during the afternoon (Fig. 5), while others interact with  $\text{NH}_3/\text{NH}_4^+$  to form NOCs,  
270 peaking during the nighttime. However, the controlling factors for these pathways could not  
271 be determined in the present study. The unexplained NOCs (~25%) might be linked to the  
272 primary emissions, such as biomass burning (Desyaterik et al., 2013). It could be partly  
273 supported by the presence of potassium and various carbon ion clusters ( $\text{C}_n^{+/-}$ ,  $n = 1, 2, 3, \dots$ )  
274 in the mass spectrum of NOCs-containing particles (Fig. 1).

275

### 276 **3.3 Seasonal variations in the observed NOCs**

277 There is a clear seasonal variation of NOCs, with higher relative contributions during  
278 summer and autumn (Figs. 3 and 4), mainly due to the variations in oxidized organics and  
279  $\text{NH}_3/\text{NH}_4^+$ . In this region, a larger contribution from secondary oxidized organics is typically  
280 observed during summer and autumn (Zhou et al., 2014; Yuan et al., 2018). The seasonal  
281 maximum  $\text{NH}_3$  concentrations have also been reported during the warmer seasons,  
282 corresponding to the peak emissions from agricultural activities and high temperatures,

---

283 while the low NH<sub>3</sub> concentrations observed in colder seasons may be attributed to gas-to-  
284 particle conversion (Pan et al., 2018; Zheng et al., 2012). Such seasonal variation in NOCs  
285 is also obtained in a model simulation, showing that the conversion of NH<sub>3</sub> into NOCs would  
286 result in a significantly higher reduction of gas-phase NH<sub>3</sub> during summer (67%) than winter  
287 (31%), due to the higher NH<sub>3</sub> and SOA concentrations present in the summer (Zhu et al.,  
288 2018). More primary NOCs may also be present during summer and autumn in the present  
289 study, due to the additional biomass burning activities in these seasons (Chen et al., 2018;  
290 Zhang et al., 2013).

291 The seasonal variations of NOCs can be adequately explained by the variations in  
292 concentrations of oxidized organics and ammonium (Fig. 4), although the hourly variations  
293 during each season are not well explained, as indicated by the lower R<sup>2</sup> values (Table S2).  
294 The correlation coefficients (R<sup>2</sup>) range from 0.24 to 0.57 for inter-seasonal variations.  
295 During spring, NOCs exhibits a limited dependence on oxidized organics (Figs. 3a and 3b),  
296 while during summer, the hourly detected number of NOCs shows a limited dependence on  
297 ammonium (Fig. 3d). These results can be explained by the PMF results, showing that the  
298 ammonium factor explained ~80% of the predicted NOCs during spring, while the oxidized  
299 organics factor dominantly contributed to the predicted NOCs during warmer seasons (Fig.  
300 S8). A detailed discussion of this issue is provided in the SI.

301

### 302 **3.4 Influence of RH and NO<sub>x</sub>**



---

303 The influence of RH on RPAs of NOCs and peak ratios of NOCs/oxidized organics, are  
304 shown in Fig. 6. While NOCs do not show a clear dependence on RH, the ratio of NOCs to  
305 oxidized organics shows a clear increase towards higher RH. This finding is consistent with  
306 the observations reported by Xu et al. (2017), in which the N/C ratio significantly increases  
307 as a function of RH in the atmosphere of Beijing. In addition, the diurnal variations of NOCs  
308 with peaks values around 20:00 are also similar to those reported by Xu et al. (2017). The  
309 peak ratios of NOCs/oxidized organics are more obviously enhanced when RH is higher than  
310 40%. These findings imply that aqueous-phase processing likely plays an important role in  
311 the formation of NOCs. Significant changes in RH, such as during the evaporation of water  
312 droplets, have been reported to facilitate the formation of NOCs via  $\text{NH}_3/\text{NH}_4^+$  and SOA  
313 (Nguyen et al., 2012). In addition, an increase in RH would improve the uptake of  $\text{NH}_3$  and  
314 formation of  $\text{NH}_4^+$ , which also contributes to the enhancement of NOCs. However, the  
315 relatively weak correlation ( $R^2 = 0.27$ ,  $p < 0.01$ ) between the peak ratios and RH, reflect the  
316 complex influence of RH on the formation of NOCs (Xu et al., 2017; Woo et al., 2013).

317 One may expect that NOCs were formed through the interactions between  $\text{NO}_x$  and  
318 oxidized organics in gas phase followed by condensation (Fry et al., 2014; Stefenelli et al.,  
319 2019; Lehtipalo et al., 2018). Low correlation coefficients ( $R^2 = 0.02\text{--}0.13$ ) between NOCs  
320 and  $\text{NO}_x$  likely indicates limited contribution of this pathways to the observed NOCs. We  
321 have also included an analysis on the relationship between peak ratios of NOCs/oxidized  
322 organics and  $\text{NO}_x$ . Peak area ratios of NOCs/oxidized organics generally increases with  
323 increasing level of  $\text{NO}_x$  (Fig. 6), but still with relatively weak correlation ( $R^2 = 0.18$ ,  $p <$

---

324 0.01). An inclusion of both NO<sub>x</sub> and RH in the above linear regression model (NOCs versus  
325 the oxidized organics and ammonium) does not improve the prediction of NOCs ( $R^2 = 0.71$ ,  
326  $p < 0.01$ ). However, it is also noted that many factors (e.g., different removal processes and  
327 lifetimes of particles vs. gasses, primary vs. secondary species, etc.) could contribute to a  
328 lack of strong correlation even if NO<sub>x</sub> did contribute to NOC formation.

329

### 330 **3.5 Atmospheric implications and limitation**

331 In this study we showed that in an urban megacity area, secondary NOCs were  
332 significantly contributed by the heterogeneous ageing of oxidized organics with NH<sub>3</sub>/NH<sub>4</sub><sup>+</sup>,  
333 providing valuable insight into SOA aging mechanisms. In particular, the effects of NH<sub>3</sub>/NH  
334 <sup>+</sup> on SOA or BrC formation remain relatively poorly understood. In the PRD region, it has  
335 been shown that oxygenated organic aerosols (OOA) account for more than 40% the total  
336 organic mass (He et al., 2011), with high concentrations of available gaseous carbonyls (Li  
337 et al., 2014). Therefore, it is expected that over half of all water soluble NOCs in this region  
338 might link to secondary processing (Yu et al., 2017). Furthermore, secondary sources have  
339 been found to contribute significantly to NOCs related BrC in Nanjing, China (Chen et al.,  
340 2018). The results presented herein also suggest that the production of NOCs might be  
341 effectively estimated by their correlation with secondary oxidized organics and ammonium.  
342 The effectiveness of correlation-based estimations needs to be examined in other regions  
343 before being generally applied in other environments. However, this approach may provide  
344 valuable insights in investigations into NOCs using atmospheric observations. In contrast, it

---

345 has previously been reported that a positive correlation exists between WSON and  
346 ammonium (Li et al., 2012), indicating similar anthropogenic sources. This divergence could  
347 be mainly attributed to varying contributions of primary sources and secondary processes to  
348 the observed NOCs. Possible future reductions in anthropogenic emissions of ammonia may  
349 reduce particle NOCs. Understanding the complex interplay between inorganic and organic  
350 nitrogen is an important part of assessing the global nitrogen cycling.

351 Moise et al. (2015) proposed that with high concentrations of reduced nitrogen  
352 compounds, high photochemical activity and frequent changes in humidity, BrC formed via  
353  $\text{NH}_3/\text{NH}_4^+$  and SOA may become a dominant contributor to aerosol absorption, specifically  
354 in agricultural and forested areas. However, this study suggests that even in typical urban  
355 areas, BrC formation via  $\text{NH}_3/\text{NH}_4^+$  and SOA should not be neglected. In particular, SOA  
356 was found to account for 44 – 71% of the organic mass in megacities across China (Huang  
357 et al., 2014), with  $\text{NH}_3$  concentrations in urban areas comparable with those from agricultural  
358 sites and 2- or 3-fold those of forested areas in China (Pan et al., 2018). Additionally, the  
359 acidic nature of particles in these regions would be also favorable for the formation of NOCs  
360 (Guo et al., 2017; Jia et al., 2018). Considering the formation of NOCs from the uptake of  
361  $\text{NH}_3$  onto SOA particles, Zhu et al. (2018) suggested that this mechanism could have a  
362 significant impact on the atmospheric concentrations of  $\text{NH}_3/\text{NH}_4^+$  and  $\text{NO}_3^-$ .

363

## 364 **5 Conclusions**

---

365 This study investigated the processes contributing to the seasonal formation of NOCs,  
366 involving ammonium and oxidized organics in urban Guangzhou, using single particle mass  
367 spectrometry. This is the first study to provide direct field observation results to confirm that  
368 the variation of NOCs correlate well and are strongly enhanced internal mixing with  
369 secondary oxidized organics. These findings highlight the possible formation pathway of  
370 NOCs through ageing of secondary oxidized organics by  $\text{NH}_3/\text{NH}_4^+$  in ambient urban  
371 environments. A clear pattern of seasonal variation in NOCs was observed, with higher  
372 relative contributions in summer and autumn as compared to spring and winter. This  
373 seasonal variation was well predicted by multiple linear regression model analysis, using the  
374 relative abundance of oxidized organics and ammonium as model inputs. More than 50% of  
375 NOCs could be explained by the interaction between oxidized organics and ammonium. The  
376 production of NOCs through such processes were facilitated by increased humidity and  $\text{NO}_x$ .  
377 These results extend our understanding of the mixing state and atmospheric processing of  
378 particulate NOCs, as well as having important implications for the accuracy of models  
379 predicting the formation, fate and impacts of NOCs in the atmosphere.

380

#### 381 **Author contribution**

382 GHZ and XHB designed the research (with input from WS, LL, ZYW, DHC, MJT, XMW  
383 and GYS), analyzed the data, and wrote the manuscript. XFL, YZF and QHL conducted air  
384 sampling work and laboratory experiments under the guidance of GHZ, XHB and XMW.  
385 All authors contributed to the refinement of the submitted manuscript.

---

386

387 **Acknowledgement**

388       This work was supported by the National Nature Science Foundation of China (No.  
389 41775124 and 41877307), the National Key Research and Development Program of China  
390 (2017YFC0210104 and 2016YFC0202204), the Science and Technology Project of  
391 Guangzhou, China (No. 201803030032), and the Guangdong Foundation for Program of  
392 Science and Technology Research (No. 2017B030314057).

---

393 **References**

394 Aiona, P. K., Lee, H. J., Leslie, R., Lin, P., Laskin, A., Laskin, J., and Nizkorodov, S. A.:  
395 Photochemistry of Products of the Aqueous Reaction of Methylglyoxal with Ammonium  
396 Sulfate, *Acs Earth Space Chem.*, 1, 522-532, doi:10.1021/acsearthspacechem.7b00075, 2017.

397 Altieri, K. E., Turpin, B. J., and Seitzinger, S. P.: Composition of Dissolved Organic  
398 Nitrogen in Continental Precipitation Investigated by Ultra-High Resolution FT-ICR Mass  
399 Spectrometry, *Environ. Sci. Technol.*, 43, 6950-6955, doi:10.1021/es9007849, 2009.

400 Andreae, M. O., and Gelencser, A.: Black carbon or brown carbon? The nature of light-  
401 absorbing carbonaceous aerosols, *Atmos. Chem. Phys.*, 6, 3131-3148, 2006.

402 Bones, D. L., Henricksen, D. K., Mang, S. A., Gonsior, M., Bateman, A. P., Nguyen, T.  
403 B., Cooper, W. J., and Nizkorodov, S. A.: Appearance of strong absorbers and fluorophores in  
404 limonene-O-3 secondary organic aerosol due to NH<sub>4</sub><sup>+</sup>-mediated chemical aging over long time  
405 scales, *J. Geophys. Res.-Atmos.*, 115, D05203, doi:10.1029/2009jd012864, 2010.

406 Cape, J. N., Cornell, S. E., Jickells, T. D., and Nemitz, E.: Organic nitrogen in the  
407 atmosphere — Where does it come from? A review of sources and methods, *Atmos. Res.*, 102,  
408 30-48, doi:10.1016/j.atmosres.2011.07.009, 2011.

409 Chen, Y., Ge, X., Chen, H., Xie, X., Chen, Y., Wang, J., Ye, Z., Bao, M., Zhang, Y., and  
410 Chen, M.: Seasonal light absorption properties of water-soluble brown carbon in atmospheric  
411 fine particles in Nanjing, China, *Atmos. Environ.*, doi:10.1016/j.atmosenv.2018.06.002, 2018.

412 Chu, B. W., Zhang, X., Liu, Y. C., He, H., Sun, Y., Jiang, J. K., Li, J. H., and Hao, J. M.:  
413 Synergetic formation of secondary inorganic and organic aerosol: effect of SO<sub>2</sub> and NH<sub>3</sub> on  
414 particle formation and growth, *Atmos. Chem. Phys.*, 16, 14219-14230, doi:10.5194/acp-16-  
415 14219-2016, 2016.

416 De Gouw, J., and Jimenez, J. L.: Organic Aerosols in the Earth's Atmosphere, *Environ.*  
417 *Sci. Technol.*, 43, 7614-7618, doi:10.1021/Es9006004, 2009.

418 De Haan, D. O., Hawkins, L. N., Kononenko, J. A., Turley, J. J., Corrigan, A. L., Tolbert,  
419 M. A., and Jimenez, J. L.: Formation of Nitrogen-Containing Oligomers by Methylglyoxal and

---

420 Amines in Simulated Evaporating Cloud Droplets, *Environ. Sci. Technol.*, 45, 984-991,  
421 doi:10.1021/es102933x, 2011.

422 De Haan, D. O., Hawkins, L. N., Welsh, H. G., Pednekar, R., Casar, J. R., Pennington, E.  
423 A., de Loera, A., Jimenez, N. G., Symons, M. A., Zauscher, M., Pajunoja, A., Caponi, L.,  
424 Cazaunau, M., Formenti, P., Gratien, A., Panguì, E., and Doussin, J.-F.: Brown Carbon  
425 Production in Ammonium- or Amine-Containing Aerosol Particles by Reactive Uptake of  
426 Methylglyoxal and Photolytic Cloud Cycling, *Environ. Sci. Technol.*, 51, 7458-7466,  
427 doi:10.1021/acs.est.7b00159, 2017.

428 De Haan, D. O., Jimenez, N. G., de Loera, A., Cazaunau, M., Gratien, A., Panguì, E., and  
429 Doussin, J.-F.: Methylglyoxal Uptake Coefficients on Aqueous Aerosol Surfaces, *J. Phys.*  
430 *Chem. A*, 122, 4854-4860, doi:10.1021/acs.jpca.8b00533, 2018.

431 Denkenberger, K. A., Moffet, R. C., Holecek, J. C., Rebotier, T. P., and Prather, K. A.:  
432 Real-time, single-particle measurements of oligomers in aged ambient aerosol particles,  
433 *Environ. Sci. Technol.*, 41, 5439-5446, doi:10.1021/es070329l, 2007.

434 Desyaterik, Y., Sun, Y., Shen, X., Lee, T., Wang, X., Wang, T., and Collett, J. L., Jr.:  
435 Speciation of "brown" carbon in cloud water impacted by agricultural biomass burning in  
436 eastern China, *J. Geophys. Res.-Atmos.*, 118, 7389-7399, doi:10.1002/jgrd.50561, 2013.

437 El-Sayed, M. M. H., Wang, Y. Q., and Hennigan, C. J.: Direct atmospheric evidence for  
438 the irreversible formation of aqueous secondary organic aerosol, *Geophys. Res. Lett.*, 42, 5577-  
439 5586, doi:10.1002/2015gl064556, 2015.

440 Feng, Y., Ramanathan, V., and Kotamarthi, V. R.: Brown carbon: a significant  
441 atmospheric absorber of solar radiation?, *Atmos. Chem. Phys.*, 13, 8607-8621,  
442 doi:10.5194/acp-13-8607-2013, 2013.

443 Fry, J. L., Draper, D. C., Barsanti, K. C., Smith, J. N., Ortega, J., Winkle, P. M., Lawler,  
444 M. J., Brown, S. S., Edwards, P. M., Cohen, R. C., and Lee, L.: Secondary Organic Aerosol  
445 Formation and Organic Nitrate Yield from NO<sub>3</sub> Oxidation of Biogenic Hydrocarbons, *Environ.*  
446 *Sci. Technol.*, 48, 11944-11953, doi:10.1021/es502204x, 2014.

---

447 Galloway, M. M., Chhabra, P. S., Chan, A. W. H., Surratt, J. D., Flagan, R. C., Seinfeld,  
448 J. H., and Keutsch, F. N.: Glyoxal uptake on ammonium sulphate seed aerosol: reaction  
449 products and reversibility of uptake under dark and irradiated conditions, *Atmos. Chem. Phys.*,  
450 9, 3331-3345, doi:10.5194/acp-9-3331-2009, 2009.

451 Gen, M., Huang, D. D., and Chan, C. K.: Reactive Uptake of Glyoxal by Ammonium-  
452 Containing Salt Particles as a Function of Relative Humidity, *Environ. Sci. Technol.*, 52, 6903-  
453 6911, doi:10.1021/acs.est.8b00606, 2018.

454 Guo, H., Xu, L., Bougiatioti, A., Cerully, K. M., Capps, S. L., Hite, J. R., Carlton, A. G.,  
455 Lee, S. H., Bergin, M. H., Ng, N. L., Nenes, A., and Weber, R. J.: Fine-particle water and pH  
456 in the southeastern United States, *Atmos. Chem. Phys.*, 15, 5211-5228, doi:10.5194/acp-15-  
457 5211-2015, 2015.

458 Guo, H., Weber, R. J., and Nenes, A.: High levels of ammonia do not raise fine particle  
459 pH sufficiently to yield nitrogen oxide-dominated sulfate production, *Sci. Rep.*, 7, 12109,  
460 doi:10.1038/s41598-017-11704-0, 2017.

461 Hawkins, L. N., Lemire, A. N., Galloway, M. M., Corrigan, A. L., Turley, J. J., Espelien,  
462 B. M., and De Haan, D. O.: Maillard Chemistry in Clouds and Aqueous Aerosol As a Source  
463 of Atmospheric Humic-Like Substances, *Environ. Sci. Technol.*, 50, 7443-7452,  
464 doi:10.1021/acs.est.6b00909, 2016.

465 He, L. Y., Huang, X. F., Xue, L., Hu, M., Lin, Y., Zheng, J., Zhang, R. Y., and Zhang, Y.  
466 H.: Submicron aerosol analysis and organic source apportionment in an urban atmosphere in  
467 Pearl River Delta of China using high-resolution aerosol mass spectrometry, *J. Geophys. Res.-*  
468 *Atmos.*, 116, 1-15, doi:10.1029/2010jd014566, 2011.

469 Healy, R. M., Sciare, J., Poulain, L., Crippa, M., Wiedensohler, A., Prevot, A. S. H.,  
470 Baltensperger, U., Sarda-Esteve, R., McGuire, M. L., Jeong, C. H., McGillicuddy, E., O'Connor,  
471 I. P., Sodeau, J. R., Evans, G. J., and Wenger, J. C.: Quantitative determination of carbonaceous  
472 particle mixing state in Paris using single-particle mass spectrometer and aerosol mass  
473 spectrometer measurements, *Atmos. Chem. Phys.*, 13, 9479-9496, doi:10.5194/acp-13-9479-  
474 2013, 2013.



---

475 Hennigan, C. J., Izumi, J., Sullivan, A. P., Weber, R. J., and Nenes, A.: A critical  
476 evaluation of proxy methods used to estimate the acidity of atmospheric particles, *Atmos. Chem.*  
477 *Phys.*, 15, 2775-2790, doi:10.5194/acp-15-2775-2015, 2015.

478 Herrmann, H., Schaefer, T., Tilgner, A., Styler, S. A., Weller, C., Teich, M., and Otto, T.:  
479 Tropospheric Aqueous-Phase Chemistry: Kinetics, Mechanisms, and Its Coupling to a  
480 Changing Gas Phase, *Chem. Rev.*, 115, 4259-4334, doi:10.1021/cr500447k, 2015.

481 Ho, K. F., Ho, S. S. H., Lee, S. C., Kawamura, K., Zou, S. C., Cao, J. J., and Xu, H. M.:  
482 Summer and winter variations of dicarboxylic acids, fatty acids and benzoic acid in PM<sub>2.5</sub> in  
483 Pearl Delta River Region, China, *Atmos. Chem. Phys.*, 11, 2197-2208, doi:10.5194/acp-11-  
484 2197-2011, 2011.

485 Ho, K. F., Ho, S. S. H., Huang, R. J., Liu, S. X., Cao, J. J., Zhang, T., Chuang, H. C., Chan,  
486 C. S., Hu, D., and Tian, L. W.: Characteristics of water-soluble organic nitrogen in fine  
487 particulate matter in the continental area of China, *Atmos. Environ.*, 106, 252-261,  
488 doi:10.1016/j.atmosenv.2015.02.010, 2015.

489 Hu, M., Wu, Z., Slanina, J., Lin, P., Liu, S., and Zeng, L.: Acidic gases, ammonia and  
490 water-soluble ions in PM<sub>2.5</sub> at a coastal site in the Pearl River Delta, China, *Atmos. Environ.*,  
491 42, 6310-6320, 2008.

492 Huang, M., Xu, J., Cai, S., Liu, X., Zhao, W., Hu, C., Gu, X., Fang, L., and Zhang, W.:  
493 Characterization of brown carbon constituents of benzene secondary organic aerosol aged with  
494 ammonia, *J. Atmos. Chem.*, 75, 205-218, doi:10.1007/s10874-017-9372-x, 2017.

495 Huang, R. J., Zhang, Y., Bozzetti, C., Ho, K. F., Cao, J. J., Han, Y., Daellenbach, K. R.,  
496 Slowik, J. G., Platt, S. M., Canonaco, F., Zotter, P., Wolf, R., Pieber, S. M., Bruns, E. A., Crippa,  
497 M., Ciarelli, G., Piazzalunga, A., Schwikowski, M., Abbaszade, G., Schnelle-Kreis, J.,  
498 Zimmermann, R., An, Z., Szidat, S., Baltensperger, U., El Haddad, I., and Prevot, A. S.: High  
499 secondary aerosol contribution to particulate pollution during haze events in China, *Nature*, 514,  
500 218-222, doi:10.1038/nature13774, 2014.

---

501 Jeong, C. H., McGuire, M. L., Godri, K. J., Slowik, J. G., Rehbein, P. J. G., and Evans, G.  
502 J.: Quantification of aerosol chemical composition using continuous single particle  
503 measurements, *Atmos. Chem. Phys.*, 11, 7027-7044, doi:10.5194/acp-11-7027-2011, 2011.

504 Jia, S. G., Sarkar, S., Zhang, Q., Wang, X. M., Wu, L. L., Chen, W. H., Huang, M. J.,  
505 Zhou, S. Z., Zhang, J. P., Yuan, L., and Yang, L. M.: Characterization of diurnal variations of  
506 PM<sub>2.5</sub> acidity using an open thermodynamic system: A case study of Guangzhou, China,  
507 *Chemosphere*, 202, 677-685, doi:10.1016/j.chemosphere.2018.03.127, 2018.

508 Kampf, C. J., Filippi, A., Zuth, C., Hoffmann, T., and Opatz, T.: Secondary brown carbon  
509 formation via the dicarbonyl imine pathway: nitrogen heterocycle formation and synergistic  
510 effects, *Phys. Chem. Chem. Phys.*, 18, 18353-18364, doi:10.1039/c6cp03029g, 2016.

511 Kanakidou, M., Seinfeld, J. H., Pandis, S. N., Barnes, I., Dentener, F. J., Facchini, M. C.,  
512 Van Dingenen, R., Ervens, B., Nenes, A., Nielsen, C. J., Swietlicki, E., Putaud, J. P., Balkanski,  
513 Y., Fuzzi, S., Horth, J., Moortgat, G. K., Winterhalter, R., Myhre, C. E. L., Tsigaridis, K.,  
514 Vignati, E., Stephanou, E. G., and Wilson, J.: Organic aerosol and global climate modelling: a  
515 review, *Atmos. Chem. Phys.*, 5, 1053-1123, 2005.

516 Kroll, J. H., Ng, N. L., Murphy, S. M., Varutbangkul, V., Flagan, R. C., and Seinfeld, J.  
517 H.: Chamber studies of secondary organic aerosol growth by reactive uptake of simple carbonyl  
518 compounds, *J. Geophys. Res.-Atmos.*, 110, doi:10.1029/2005JD006004, 2005.

519 Laskin, A., Smith, J. S., and Laskin, J.: Molecular Characterization of Nitrogen-  
520 Containing Organic Compounds in Biomass Burning Aerosols Using High-Resolution Mass  
521 Spectrometry, *Environ. Sci. Technol.*, 43, 3764-3771, doi:10.1021/es803456n, 2009.

522 Laskin, A., Laskin, J., and Nizkorodov, S. A.: Chemistry of Atmospheric Brown Carbon,  
523 *Chem. Rev.*, 115, 4335-4382, doi:10.1021/cr5006167, 2015.

524 Lee, A. K. Y., Zhao, R., Li, R., Liggi, J., Li, S. M., and Abbatt, J. P. D.: Formation of  
525 Light Absorbing Organo-Nitrogen Species from Evaporation of Droplets Containing Glyoxal  
526 and Ammonium Sulfate, *Environ. Sci. Technol.*, 47, 12819-12826, doi:10.1021/es402687w,  
527 2013.

---

528 Lee, S. H., Murphy, D. M., Thomson, D. S., and Middlebrook, A. M.: Nitrate and oxidized  
529 organic ions in single particle mass spectra during the 1999 Atlanta Supersite Project, *J.*  
530 *Geophys. Res.*, 108, 8417, doi:10.1029/2001jd001455, 2003.

531 Lehtipalo, K., Yan, C., Dada, L., Bianchi, F., Xiao, M., Wagner, R., Stolzenburg, D.,  
532 Ahonen, L. R., Amorim, A., Baccarini, A., Bauer, P. S., Baumgartner, B., Bergen, A.,  
533 Bernhammer, A.-K., Breitenlechner, M., Brilke, S., Buchholz, A., Mazon, S. B., Chen, D., Chen,  
534 X., Dias, A., Dommen, J., Draper, D. C., Duplissy, J., Ehn, M., Finkenzeller, H., Fischer, L.,  
535 Frege, C., Fuchs, C., Garmash, O., Gordon, H., Hakala, J., He, X., Heikkinen, L., Heinritzi, M.,  
536 Helm, J. C., Hofbauer, V., Hoyle, C. R., Jokinen, T., Kangasluoma, J., Kerminen, V.-M., Kim,  
537 C., Kirkby, J., Kontkanen, J., Kürten, A., Lawler, M. J., Mai, H., Mathot, S., Mauldin, R. L.,  
538 Molteni, U., Nichman, L., Nie, W., Nieminen, T., Ojdanic, A., Onnela, A., Passananti, M.,  
539 Petäjä, T., Piel, F., Pospisilova, V., Quéléver, L. L. J., Rissanen, M. P., Rose, C., Sarnela, N.,  
540 Schallhart, S., Schuchmann, S., Sengupta, K., Simon, M., Sipilä, M., Tauber, C., Tomé, A.,  
541 Tröstl, J., Väisänen, O., Vogel, A. L., Volkamer, R., Wagner, A. C., Wang, M., Weitz, L.,  
542 Wimmer, D., Ye, P., Ylisirniö, A., Zha, Q., Carslaw, K. S., Curtius, J., Donahue, N. M., Flagan,  
543 R. C., Hansel, A., Riipinen, I., Virtanen, A., Winkler, P. M., Baltensperger, U., Kulmala, M.,  
544 and Worsnop, D. R.: Multicomponent new particle formation from sulfuric acid, ammonia, and  
545 biogenic vapors, *Sci. Adv.*, 4, eaau5363, doi:10.1126/sciadv.aau5363, 2018.

546 Li, J., Fang, Y. T., Yoh, M., Wang, X. M., Wu, Z. Y., Kuang, Y. W., and Wen, D. Z.:  
547 Organic nitrogen deposition in precipitation in metropolitan Guangzhou city of southern China,  
548 *Atmos. Res.*, 113, 57-67, doi:10.1016/j.atmosres.2012.04.019, 2012.

549 Li, L., Huang, Z. X., Dong, J. G., Li, M., Gao, W., Nian, H. Q., Fu, Z., Zhang, G. H., Bi,  
550 X. H., Cheng, P., and Zhou, Z.: Real time bipolar time-of-flight mass spectrometer for analyzing  
551 single aerosol particles, *Intl. J. Mass. Spectrom.*, 303, 118-124, doi:10.1016/j.ijms.2011.01.017,  
552 2011.

553 Li, X., Rohrer, F., Brauers, T., Hofzumahaus, A., Lu, K., Shao, M., Zhang, Y. H., and  
554 Wahner, A.: Modeling of HCHO and CHOCHO at a semi-rural site in southern China during

---

555 the PRIDE-PRD2006 campaign, *Atmos. Chem. Phys.*, 14, 12291-12305, doi:10.5194/acp-14-  
556 12291-2014, 2014.

557 Li, Z. J., Nizkorodov, S. A., Chen, H., Lu, X. H., Yang, X., and Chen, J. M.: Nitrogen-  
558 containing secondary organic aerosol formation by acrolein reaction with ammonia/ammonium,  
559 *Atmos. Chem. Phys.*, 19, 1343-1356, doi:10.5194/acp-19-1343-2019, 2019.

560 Liggio, J., Li, S. M., and McLaren, R.: Reactive uptake of glyoxal by particulate matter, *J.*  
561 *Geophys. Res.-Atmos.*, 110, doi:10.1029/2004jd005113, 2005.

562 Lin, P., Aiona, P. K., Li, Y., Shiraiwa, M., Laskin, J., Nizkorodov, S. A., and Laskin, A.:  
563 Molecular Characterization of Brown Carbon in Biomass Burning Aerosol Particles, *Environ.*  
564 *Sci. Technol.*, 50, 11815-11824, doi:10.1021/acs.est.6603024, 2016.

565 Liu, Y., Liggio, J., Staebler, R., and Li, S. M.: Reactive uptake of ammonia to secondary  
566 organic aerosols: kinetics of organonitrogen formation, *Atmos. Chem. Phys.*, 15, 13569-13584,  
567 doi:10.5194/acp-15-13569-2015, 2015.

568 Mace, K. A., Kubilay, N., and Duce, R. A.: Organic nitrogen in rain and aerosol in the  
569 eastern Mediterranean atmosphere: An association with atmospheric dust, *J. Geophys. Res.-*  
570 *Atmos.*, 108, doi:10.1029/2002jd002997, 2003.

571 Mang, S. A., Henricksen, D. K., Bateman, A. P., Andersen, M. P. S., Blake, D. R., and  
572 Nizkorodov, S. A.: Contribution of Carbonyl Photochemistry to Aging of Atmospheric  
573 Secondary Organic Aerosol, *J. Phys. Chem. A*, 112, 8337-8344, doi:10.1021/jp804376c, 2008.

574 Miyazaki, Y., Fu, P. Q., Ono, K., Tachibana, E., and Kawamura, K.: Seasonal cycles of  
575 water-soluble organic nitrogen aerosols in a deciduous broadleaf forest in northern Japan, *J.*  
576 *Geophys. Res.-Atmos.*, 119, 1440-1454, doi:10.1002/2013JD020713, 2014.

577 Mohr, C., Lopez-Hilfiker, F. D., Zotter, P., Prévôt, A. S. H., Xu, L., Ng, N. L., Herndon,  
578 S. C., Williams, L. R., Franklin, J. P., Zahniser, M. S., Worsnop, D. R., Knighton, W. B., Aiken,  
579 A. C., Gorkowski, K. J., Dubey, M. K., Allan, J. D., and Thornton, J. A.: Contribution of  
580 Nitrated Phenols to Wood Burning Brown Carbon Light Absorption in Detling, United  
581 Kingdom during Winter Time, *Environ. Sci. Technol.*, 47, 6316-6324, doi:10.1021/es400683v,  
582 2013.

---

583 Moise, T., Flores, J. M., and Rudich, Y.: Optical Properties of Secondary Organic Aerosols  
584 and Their Changes by Chemical Processes, *Chem. Rev.*, 115, 4400-4439,  
585 doi:10.1021/cr5005259, 2015.

586 Murphy, J. G., Gregoire, P. K., Tevlin, A. G., Wentworth, G. R., Ellis, R. A., Markovic,  
587 M. Z., and VandenBoer, T. C.: Observational constraints on particle acidity using  
588 measurements and modelling of particles and gases, *Faraday Discuss.*, 200, 379-395,  
589 doi:10.1039/c7fd00086c, 2017.

590 Neff, J. C., Holland, E. A., Dentener, F. J., McDowell, W. H., and Russell, K. M.: The  
591 origin, composition and rates of organic nitrogen deposition: A missing piece of the nitrogen  
592 cycle?, *Biogeochemistry*, 57, 99-136, 2002.

593 Nguyen, T. B., Lee, P. B., Updyke, K. M., Bones, D. L., Laskin, J., Laskin, A., and  
594 Nizkorodov, S. A.: Formation of nitrogen- and sulfur-containing light-absorbing compounds  
595 accelerated by evaporation of water from secondary organic aerosols, *J. Geophys. Res.-Atmos.*,  
596 117, D01207, doi:10.1029/2011jd016944, 2012.

597 Norris, G., Vedantham, R., Wade, K., Zahn, P., Brown, S., Paatero, P., Eberly, S., and  
598 Foley, C. (2009), Guidance document for PMF applications with the Multilinear Engine, edited,  
599 Prepared for the U.S. Environmental Protection Agency, Research Triangle Park, NC.

600 Noziere, B., Dziedzic, P., and Cordova, A.: Products and Kinetics of the Liquid-Phase  
601 Reaction of Glyoxal Catalyzed by Ammonium Ions (NH<sub>4</sub><sup>+</sup>), *J. Phys. Chem. A*, 113, 231-237,  
602 doi:10.1021/jp8078293, 2009.

603 Noziere, B., Kaberer, M., Claeys, M., Allan, J., D'Anna, B., Decesari, S., Finessi, E.,  
604 Glasius, M., Grgic, I., Hamilton, J. F., Hoffmann, T., Iinuma, Y., Jaoui, M., Kahno, A., Kampf,  
605 C. J., Kourtchev, I., Maenhaut, W., Marsden, N., Saarikoski, S., Schnelle-Kreis, J., Surratt, J.  
606 D., Szidat, S., Szmigielski, R., and Wisthaler, A.: The Molecular Identification of Organic  
607 Compounds in the Atmosphere: State of the Art and Challenges, *Chem. Rev.*, 115, 3919-3983,  
608 doi:10.1021/cr5003485, 2015.

609 Pagels, J., Dutcher, D. D., Stolzenburg, M. R., McMurry, P. H., Galli, M. E., and Gross,  
610 D. S.: Fine-particle emissions from solid biofuel combustion studied with single-particle mass

---

611 spectrometry: Identification of markers for organics, soot, and ash components, *J. Geophys.*  
612 *Res.-Atmos.*, 118, 859-870, doi:10.1029/2012jd018389, 2013.

613 Pan, Y. P., Tian, S. L., Zhao, Y. H., Zhang, L., Zhu, X. Y., Gao, J., Huang, W., Zhou, Y.  
614 B., Song, Y., Zhang, Q., and Wang, Y. S.: Identifying Ammonia Hotspots in China Using a  
615 National Observation Network, *Environ. Sci. Technol.*, 52, 3926-3934,  
616 doi:10.1021/acs.est.7b05235, 2018.

617 Paulot, F., Wunch, D., Crouse, J. D., Toon, G. C., Millet, D. B., DeCarlo, P. F.,  
618 Vigouroux, C., Deutscher, N. M., González Abad, G., Notholt, J., Warneke, T., Hannigan, J.  
619 W., Warneke, C., de Gouw, J. A., Dunlea, E. J., De Mazière, M., Griffith, D. W. T., Bernath,  
620 P., Jimenez, J. L., and Wennberg, P. O.: Importance of secondary sources in the atmospheric  
621 budgets of formic and acetic acids, *Atmos. Chem. Phys.*, 11, 1989-2013, doi:10.5194/acp-11-  
622 1989-2011, 2011.

623 Qin, X. Y., Bhave, P. V., and Prather, K. A.: Comparison of two methods for obtaining  
624 quantitative mass concentrations from aerosol time-of-flight mass spectrometry measurements,  
625 *Anal. Chem.*, 78, 6169-6178, doi:10.1021/ac060395q, 2006.

626 Rastogi, N., Zhang, X., Edgerton, E. S., Ingall, E., and Weber, R. J.: Filterable water-  
627 soluble organic nitrogen in fine particles over the southeastern USA during summer, *Atmos.*  
628 *Environ.*, 45, 6040-6047, doi:10.1016/j.atmosenv.2011.07.045, 2011.

629 Sareen, N., Schwier, A. N., Shapiro, E. L., Mitroo, D., and McNeill, V. F.: Secondary  
630 organic material formed by methylglyoxal in aqueous aerosol mimics, *Atmos. Chem. Phys.*, 10,  
631 997-1016, doi:10.5194/acp-10-997-2010, 2010.

632 Shapiro, E. L., Szprengiel, J., Sareen, N., Jen, C. N., Giordano, M. R., and McNeill, V. F.:  
633 Light-absorbing secondary organic material formed by glyoxal in aqueous aerosol mimics,  
634 *Atmos. Chem. Phys.*, 9, 2289-2300, 2009.

635 Shi, J., Gao, H., Qi, J., Zhang, J., and Yao, X.: Sources, compositions, and distributions of  
636 water-soluble organic nitrogen in aerosols over the China Sea, *J. Geophys. Res.-Atmos.*, 115,  
637 doi:10.1029/2009jd013238, 2010.

---

638 Shrivastava, M., Cappa, C. D., Fan, J. W., Goldstein, A. H., Guenther, A. B., Jimenez, J.  
639 L., Kuang, C., Laskin, A., Martin, S. T., Ng, N. L., Petaja, T., Pierce, J. R., Rasch, P. J., Roldin,  
640 P., Seinfeld, J. H., Shilling, J., Smith, J. N., Thornton, J. A., Volkamer, R., Wang, J., Worsnop,  
641 D. R., Zaveri, R. A., Zelenyuk, A., and Zhang, Q.: Recent advances in understanding secondary  
642 organic aerosol: Implications for global climate forcing, *Rev. Geophys.*, 55, 509-559,  
643 doi:10.1002/2016RG000540, 2017.

644 Silva, P. J., and Prather, K. A.: Interpretation of mass spectra from organic compounds in  
645 aerosol time-of-flight mass spectrometry, *Anal. Chem.*, 72, 3553-3562, 2000.

646 Stefenelli, G., Pospisilova, V., Lopez-Hilfiker, F. D., Daellenbach, K. R., Hüglin, C., Tong,  
647 Y., Baltensperger, U., Prevot, A. S. H., and Slowik, J. G.: Organic aerosol source apportionment  
648 in Zurich using extractive electrospray ionization time-of-flight mass spectrometry (EESI-TOF):  
649 Part I, biogenic influences and day/night chemistry in summer, *Atmos. Chem. Phys. Discuss.*,  
650 2019, 1-36, doi:10.5194/acp-2019-361, 2019.

651 Sullivan, R. C., and Prather, K. A.: Investigations of the diurnal cycle and mixing state of  
652 oxalic acid in individual particles in Asian aerosol outflow, *Environ. Sci. Technol.*, 41, 8062-  
653 8069, 2007.

654 Sun, J. Z., Zhi, G. R., Hitznerberger, R., Chen, Y. J., Tian, C. G., Zhang, Y. Y., Feng, Y.  
655 L., Cheng, M. M., Zhang, Y. Z., Cai, J., Chen, F., Qiu, Y., Jiang, Z., Li, J., Zhang, G., and Mo,  
656 Y.: Emission factors and light absorption properties of brown carbon from household coal  
657 combustion in China, *Atmos. Chem. Phys.*, 17, 4769-4780, doi:10.5194/acp-17-4769-2017,  
658 2017.

659 Sun, Y. L., Zhang, Q., Schwab, J. J., Demerjian, K. L., Chen, W. N., Bae, M. S., Hung, H.  
660 M., Hogrefe, O., Frank, B., Rattigan, O. V., and Lin, Y. C.: Characterization of the sources and  
661 processes of organic and inorganic aerosols in New York city with a high-resolution time-of-  
662 flight aerosol mass spectrometer, *Atmos. Chem. Phys.*, 11, 1581-1602, doi:10.5194/acp-11-  
663 1581-2011, 2011.

---

664 Updyke, K. M., Nguyen, T. B., and Nizkorodov, S. A.: Formation of brown carbon via  
665 reactions of ammonia with secondary organic aerosols from biogenic and anthropogenic  
666 precursors, *Atmos. Environ.*, 63, 22-31, doi:10.1016/j.atmosenv.2012.09.012, 2012.

667 Wang, X. F., Gao, S., Yang, X., Chen, H., Chen, J. M., Zhuang, G. S., Surratt, J. D., Chan,  
668 M. N., and Seinfeld, J. H.: Evidence for High Molecular Weight Nitrogen-Containing Organic  
669 Salts in Urban Aerosols, *Environ. Sci. Technol.*, 44, 4441-4446, 2010.

670 Wang, X. F., Wang, H. L., Jing, H., Wang, W. N., Cui, W. D., Williams, B. J., and Biswas,  
671 P.: Formation of Nitrogen-Containing Organic Aerosol during Combustion of High-Sulfur-  
672 Content Coal, *Energ. Fuel.*, 31, 14161-14168, doi:10.1021/acs.energyfuels.7b02273, 2017.

673 Woo, J. L., Kim, D. D., Schwier, A. N., Li, R. Z., and McNeill, V. F.: Aqueous aerosol  
674 SOA formation: impact on aerosol physical properties, *Faraday Discuss.*, 165, 357-367,  
675 doi:10.1039/c3fd00032j, 2013.

676 Xu, W. Q., Sun, Y. L., Wang, Q. Q., Du, W., Zhao, J., Ge, X. L., Han, T. T., Zhang, Y. J.,  
677 Zhou, W., Li, J., Fu, P. Q., Wang, Z. F., and Worsnop, D. R.: Seasonal Characterization of  
678 Organic Nitrogen in Atmospheric Aerosols Using High Resolution Aerosol Mass Spectrometry  
679 in Beijing, China, *Acs Earth Space Chem.*, 1, 673-682,  
680 doi:10.1021/acsearthspacechem.7b00106, 2017.

681 Yan, J., Wang, X., Gong, P., Wang, C., and Cong, Z.: Review of brown carbon aerosols:  
682 Recent progress and perspectives, *Sci. Total. Environ.*, 634, 1475-1485,  
683 doi:10.1016/j.scitotenv.2018.04.083, 2018.

684 Yu, X., Yu, Q. Q., Zhu, M., Tang, M. J., Li, S., Yang, W. Q., Zhang, Y. L., Deng, W., Li,  
685 G. H., Yu, Y. G., Huang, Z. H., Song, W., Ding, X., Hu, Q. H., Li, J., Bi, X. H., and Wang, X.  
686 M.: Water Soluble Organic Nitrogen (WSO<sub>N</sub>) in Ambient Fine Particles Over a Megacity in  
687 South China: Spatiotemporal Variations and Source Apportionment, *J. Geophys. Res.-Atmos.*,  
688 122, 13045-13060, doi:10.1002/2017JD027327, 2017.

689 Yuan, B., Liggiio, J., Wentzell, J., Li, S. M., Stark, H., Roberts, J. M., Gilman, J., Lerner,  
690 B., Warneke, C., Li, R., Leithead, A., Osthoff, H. D., Wild, R., Brown, S. S., and de Gouw, J.  
691 A.: Secondary formation of nitrated phenols: insights from observations during the Uintah



---

692 Basin Winter Ozone Study (UBWOS) 2014, *Atmos. Chem. Phys.*, 16, 2139-2153,  
693 doi:10.5194/acp-16-2139-2016, 2016.

694 Yuan, Q., Lai, S., Song, J., Ding, X., Zheng, L., Wang, X., Zhao, Y., Zheng, J., Yue, D.,  
695 Zhong, L., Niu, X., and Zhang, Y.: Seasonal cycles of secondary organic aerosol tracers in rural  
696 Guangzhou, Southern China: The importance of atmospheric oxidants, *Environ. Pollut.*, 240,  
697 884-893, doi:10.1016/j.envpol.2018.05.009, 2018.

698 Zauscher, M. D., Wang, Y., Moore, M. J. K., Gaston, C. J., and Prather, K. A.: Air Quality  
699 Impact and Physicochemical Aging of Biomass Burning Aerosols during the 2007 San Diego  
700 Wildfires, *Environ. Sci. Technol.*, 47, 7633-7643, doi:10.1021/es4004137, 2013.

701 Zawadowicz, M. A., Froyd, K. D., Murphy, D. M., and Cziczo, D. J.: Improved  
702 identification of primary biological aerosol particles using single-particle mass spectrometry,  
703 *Atmos. Chem. Phys.*, 17, 7193-7212, doi:10.5194/acp-17-7193-2017, 2017.

704 Zhang, G., Lin, Q., Peng, L., Yang, Y., Jiang, F., Liu, F., Song, W., Chen, D., Cai, Z., Bi,  
705 X., Miller, M., Tang, M., Huang, W., Wang, X., Peng, P., and Sheng, G.: Oxalate Formation  
706 Enhanced by Fe-Containing Particles and Environmental Implications, *Environ. Sci. Technol.*,  
707 53, 1269-1277, doi:10.1021/acs.est.8b05280, 2019.

708 Zhang, G. H., Bi, X. H., He, J. J., Chen, D. H., Chan, L. Y., Xie, G. W., Wang, X. M.,  
709 Sheng, G. Y., Fu, J. M., and Zhou, Z.: Variation of secondary coatings associated with  
710 elemental carbon by single particle analysis, *Atmos. Environ.*, 92, 162-170,  
711 doi:10.1016/j.atmosenv.2014.04.018, 2014.

712 Zhang, G. H., Lin, Q. H., Peng, L., Yang, Y. X., Fu, Y. Z., Bi, X. H., Li, M., Chen, D. H.,  
713 Chen, J. X., Cai, Z., Wang, X. M., Peng, P. A., Sheng, G. Y., and Zhou, Z.: Insight into the in-  
714 cloud formation of oxalate based on in situ measurement by single particle mass spectrometry,  
715 *Atmos. Chem. Phys.*, 17, 13891-13901, doi:10.5194/acp-17-13891-2017, 2017.

716 Zhang, Q., Duan, F., He, K., Ma, Y., Li, H., Kimoto, T., and Zheng, A.: Organic nitrogen  
717 in PM<sub>2.5</sub> in Beijing, *Frontiers of Environmental Science & Engineering*, 9, 1004-1014,  
718 doi:10.1007/s11783-015-0799-5, 2015.

---

719 Zhang, Y. S., Shao, M., Lin, Y., Luan, S. J., Mao, N., Chen, W. T., and Wang, M.:  
720 Emission inventory of carbonaceous pollutants from biomass burning in the Pearl River Delta  
721 Region, China, *Atmos. Environ.*, 76, 189-199, doi:10.1016/j.atmosenv.2012.05.055, 2013.

722 Zhao, R., Lee, A. K. Y., and Abbatt, J. P. D.: Investigation of Aqueous-Phase  
723 Photooxidation of Glyoxal and Methylglyoxal by Aerosol Chemical Ionization Mass  
724 Spectrometry: Observation of Hydroxyhydroperoxide Formation, *J. Phys. Chem. A*, 116, 6253-  
725 6263, doi:10.1021/jp211528d, 2012.

726 Zhao, R., Lee, A. K. Y., Huang, L., Li, X., Yang, F., and Abbatt, J. P. D.: Photochemical  
727 processing of aqueous atmospheric brown carbon, *Atmos. Chem. Phys.*, 15, 6087-6100,  
728 doi:10.5194/acp-15-6087-2015, 2015.

729 Zheng, J. Y., Yin, S. S., Kang, D. W., Che, W. W., and Zhong, L. J.: Development and  
730 uncertainty analysis of a high-resolution NH<sub>3</sub> emissions inventory and its implications with  
731 precipitation over the Pearl River Delta region, China, *Atmos. Chem. Phys.*, 12, 7041-7058,  
732 doi:10.5194/acp-12-7041-2012, 2012.

733 Zhou, S. Z., Wang, T., Wang, Z., Li, W. J., Xu, Z., Wang, X. F., Yuan, C., Poon, C. N.,  
734 Louie, P. K. K., Luk, C. W. Y., and Wang, W. X.: Photochemical evolution of organic aerosols  
735 observed in urban plumes from Hong Kong and the Pearl River Delta of China, *Atmos. Environ.*,  
736 88, 219-229, doi:10.1016/j.atmosenv.2014.01.032, 2014.

737 Zhou, Y., Huang, X. H. H., Griffith, S. M., Li, M., Li, L., Zhou, Z., Wu, C., Meng, J. W.,  
738 Chan, C. K., Louie, P. K. K., and Yu, J. Z.: A field measurement based scaling approach for  
739 quantification of major ions, organic carbon, and elemental carbon using a single particle  
740 aerosol mass spectrometer, *Atmos. Environ.*, 143, 300-312,  
741 doi:10.1016/j.atmosenv.2016.08.054, 2016.

742 Zhu, S. P., Horne, J. R., Montoya-Aguilera, J., Hinks, M. L., Nizkorodov, S. A., and  
743 Dabdub, D.: Modeling reactive ammonia uptake by secondary organic aerosol in CMAQ:  
744 application to the continental US, *Atmos. Chem. Phys.*, 18, 3641-3657, doi:10.5194/acp-18-  
745 3641-2018, 2018.

746

747 **Figure captions**

748 Figure 1. Representative mass spectrum for NOCs-containing particles. The ion  
749 peaks corresponding to NOCs and oxidized organics are highlighted with red bars.

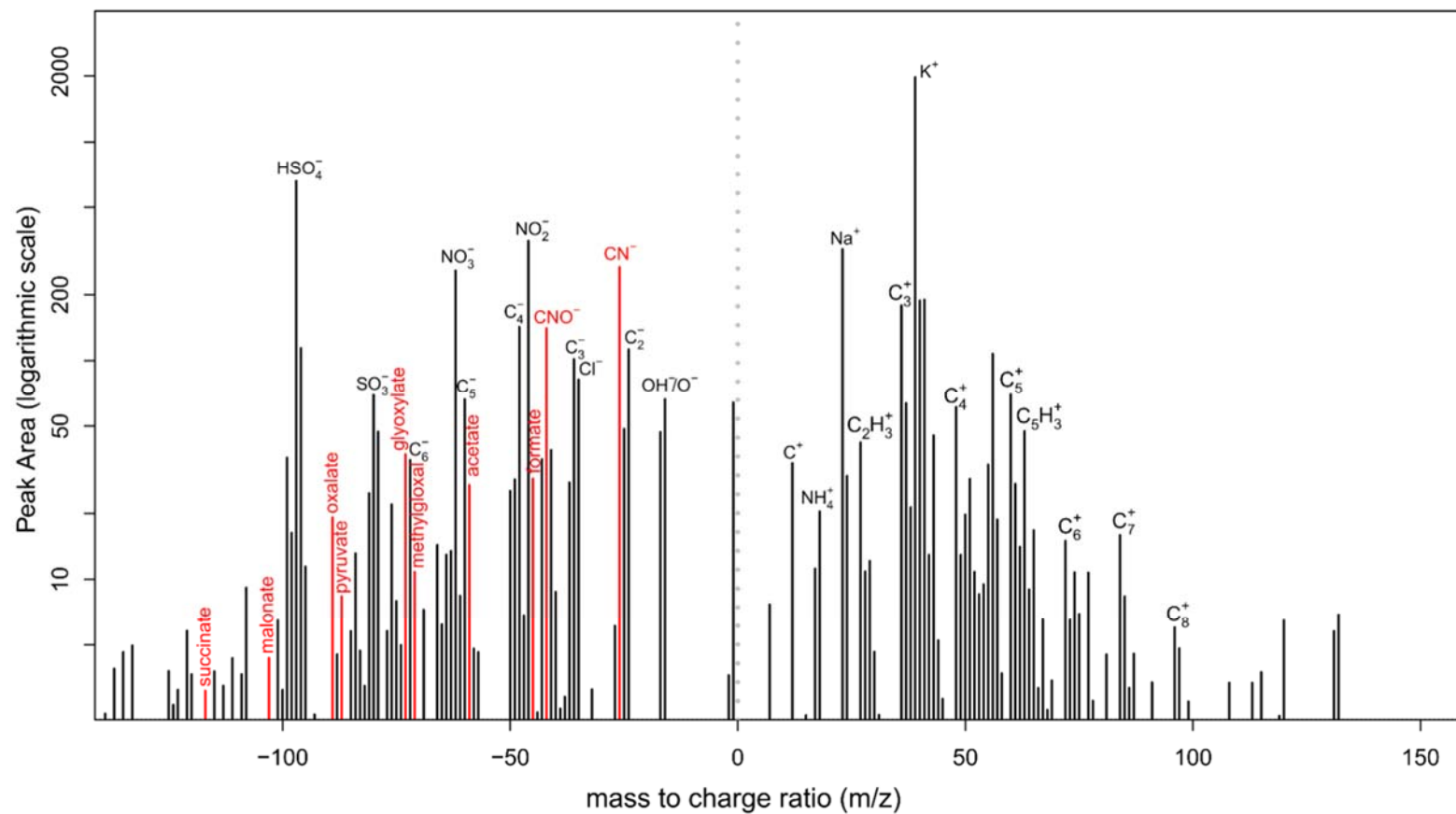
750 Figure 2. The variation in hourly mean Nfs of the oxidized organics and  
751 ammonium that internally mixed with NOCs. Box and whisker plot shows lower,  
752 median and upper lines, denoting the 25<sup>th</sup>, 50<sup>th</sup> and 75<sup>th</sup> percentiles, respectively; the  
753 lower and upper edges denote the 10<sup>th</sup> and 90<sup>th</sup> percentiles, respectively.

754 Figure 3. Correlation analysis of (a, c) the RPAs and (b, d) the number of  
755 detected NOCs, with the oxidized organics and ammonium in different seasons.  
756 Significant ( $p < 0.01$ ) correlations were obtained for both the total observed data and  
757 the seasonally separated data. RPA is defined as the fractional peak area of each  $m/z$   
758 relative to the sum of peak areas in the mass spectrum and is applied to represent the  
759 relative amount of a species on a particle (Jeong et al., 2011; Healy et al., 2013).

760 Figure 4. Comparison between the measured and predicted RPAs for NOCs.

761 Figure 5. (left) PMF-resolved 3-factor source profiles (percentage of total species)  
762 and (right) their diurnal variation (arbitrary unit).

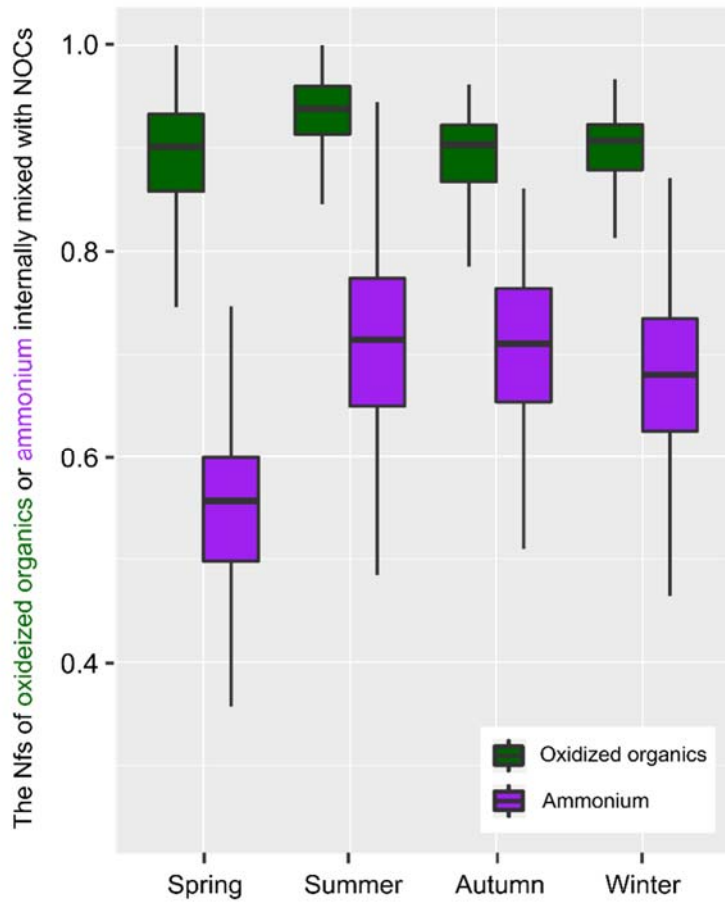
763 Figure 6. The dependence of NOCs and the ratio of NOCs to the oxidized organics  
764 on RH.



765

766

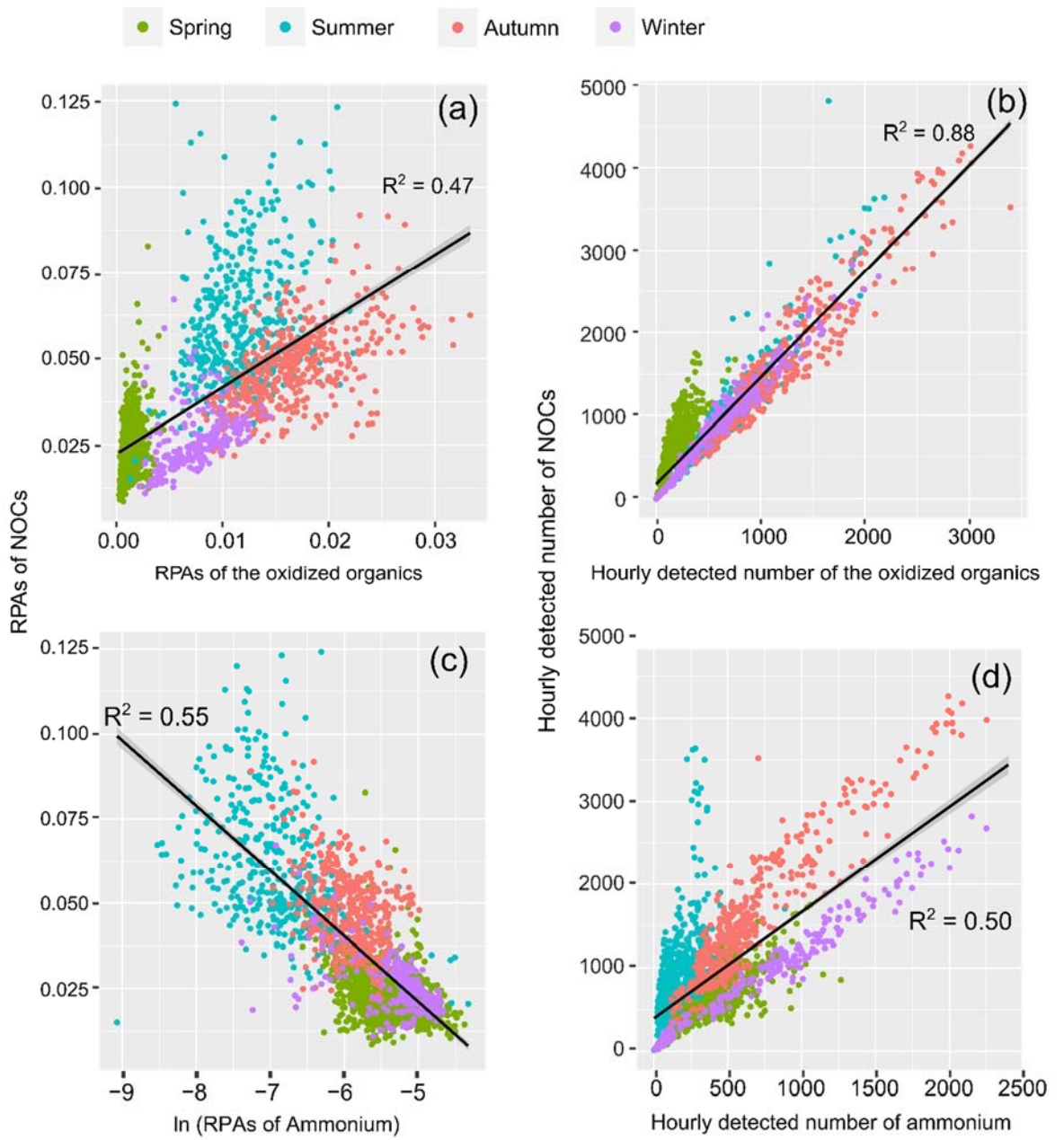
Fig. 1.



767

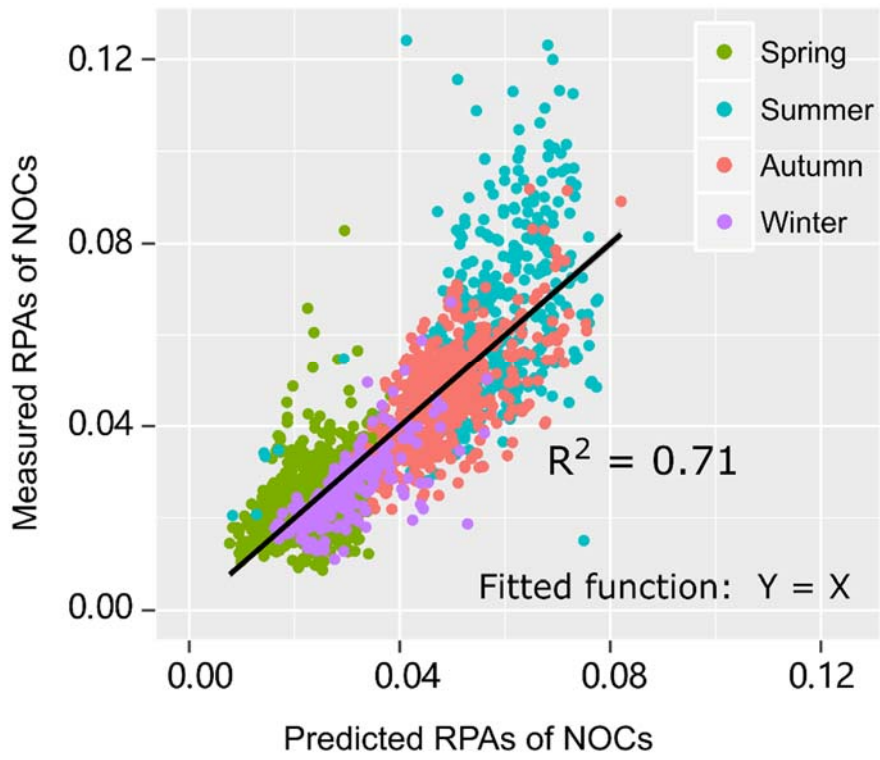
768

Fig. 2.



769

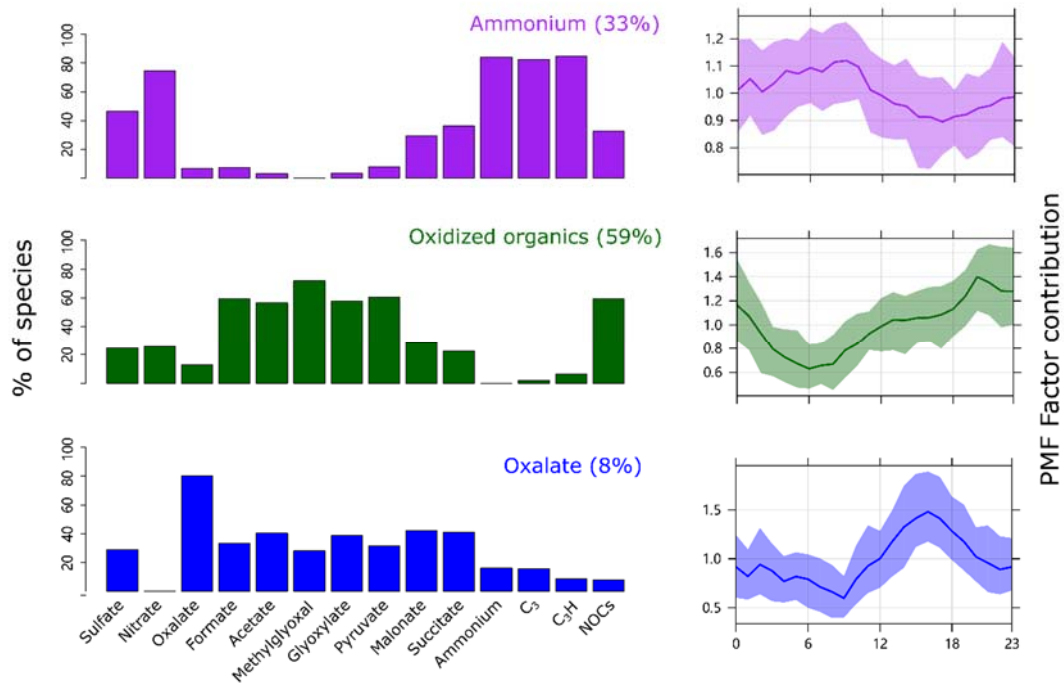
770 Fig. 3.



771

772 **Fig. 4.**

773

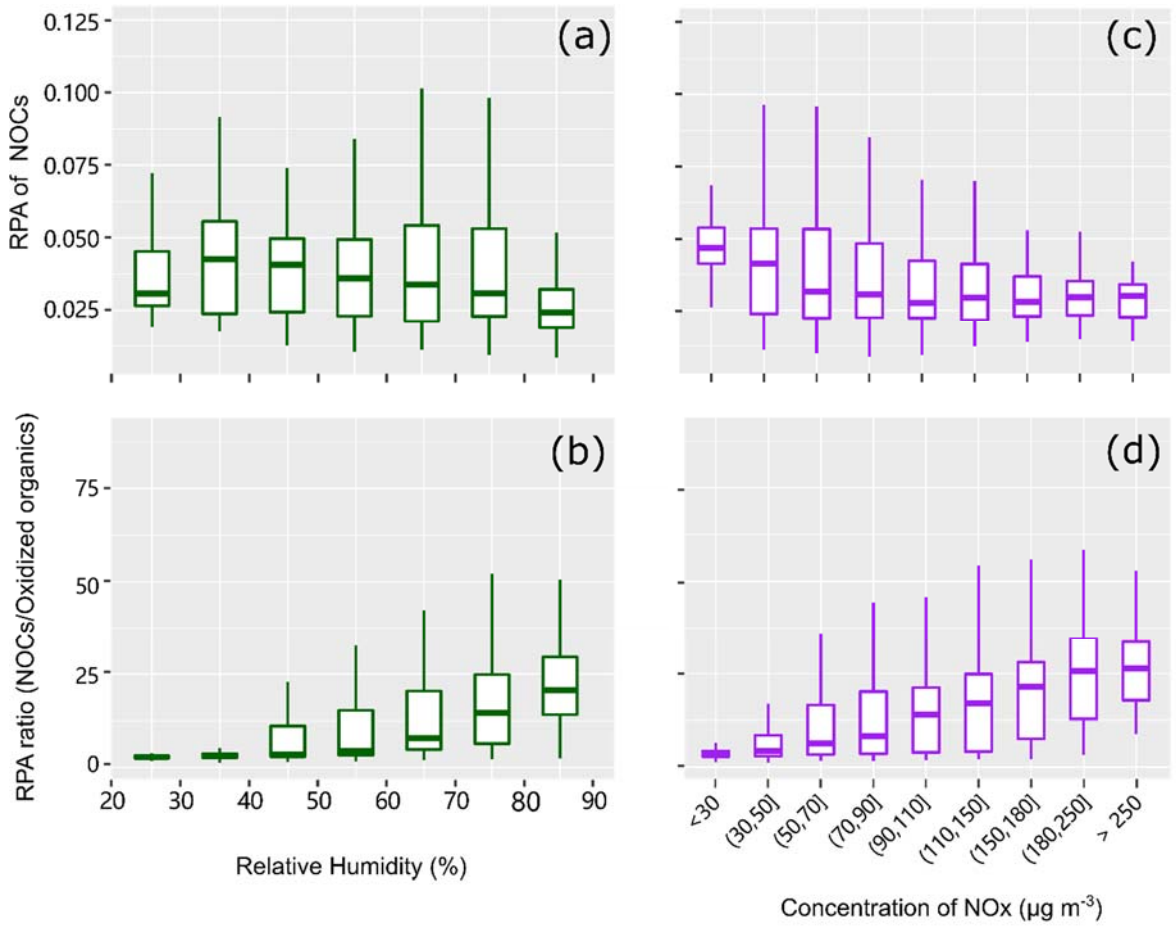


774

775

Fig. 5.





776

777

**Fig. 6.**